

A multi-element detector array for heavy fragments emitted in intermediate energy nuclear reactions

I. Iori, L. Manduci, A. Moroni, R. Scardaoni, Sun ChongWen^a, Zhang Yuzhao^b, Zhang Guangming^a, F. Giglio, E. Mora, G. Di Pietro, L. Delleria, A. Cortesi, R. Bassini, C. Boiano, S. Brambilla and M. Malatesta

Dipartimento di Fisica dell'Università and Istituto Nazionale di Fisica Nucleare, Milano, Italy

M. Bruno, M. D'Agostino, M.L. Fiandri, E. Fuschini, P.M. Milazzo and G. Busacchi

Dipartimento di Fisica dell'Università and Istituto Nazionale di Fisica Nucleare, Bologna, Italy

A. Cunsolo, A. Foti, C. Gianino and G. Sava

Dipartimento di Fisica dell'Università and Istituto Nazionale di Fisica Nucleare, Catania, Italy

F. Gramegna

Istituto Nazionale di Fisica Nucleare, Laboratori Nazionali di Legnaro, Legnaro, Italy

P. Buttazzo, G.V. Margagliotti and G. Vannini

Dipartimento di Fisica dell'Università and Istituto Nazionale di Fisica Nucleare, Trieste, Italy

G. Auger and E. Plagnol

GANIL, Caen, France

Received 7 September 1992

To investigate complex fragment emission in intermediate energy nucleus–nucleus collisions, an array of three-element telescopes has been constructed. The array is designed to measure energy, charge and emission angles of fragments with Z values from 2 up to the projectile atomic number when studying reactions in reverse kinematics. In this case it has a good efficiency even for events with complex fragment high multiplicity. Each telescope is made of an ionization chamber (filled with CF_4 at a pressure up to 300 mbar), a Si detector (500 μm thick, position sensitive in two dimensions) and a CsI(Tl) scintillator with photodiode readout.

1. Introduction

In heavy-ion reactions at intermediate energy (20–100 A MeV) the emission of complex fragments is an interesting problem, widely investigated both from the theoretical and the experimental point of view, being relied to the behaviour of nuclei at high temperature and density.

From the experimental side, it is necessary to detect and identify complex fragments in a large range of Z values and energies with an energy threshold as low as possible. Furthermore it is necessary to cover the complete 4π solid angle with a detector of suitable granularity, to obtain the correct fragment multiplicity value. In recent years different detector arrays have been constructed satisfying these requirements more or less [1–9].

In this paper we describe a detector array conceived to detect mainly intermediate mass fragments (IMF) and with a good angular coverage if used in reverse kinematics reactions. In fact in this case, due to the

^a Academia Sinica, Shanghai, China.

^b Academia Sinica, Lanzhou, China.

large center of mass velocity, most of the reaction products are emitted, in the laboratory system, within a forward cone so that a good angular coverage can be achieved with a detector of limited size and cost. A further advantage of the fragment high velocity, is an easier Z identification.

The detector array granularity has to be adequate to give the correct multiplicity distribution. In fact distortions of the multiplicity distribution can be introduced by the loss of coincident events because of the geometry and unavoidable dead space in the array, or because of multiple hits, or because of one particle hitting more than one detector. A relationship between the event multiplicity and the number of detectors, may be established with some simple assumption. At the energies and nuclear systems we are interested in, assuming a maximum value of 10 for the IMF multiplicity, taking into account the geometrical efficiency, accepting a multiple detection probability less than 10% and disregarding the probability that a particle can be scattered from one detector to another, a total number of detectors [9] of around 50 is deduced.

The detection system here described is designed to satisfy these requirements: high granularity for heavy fragments, high geometrical efficiency within the covered solid angle, very low energy threshold and good position determination. Furthermore, each telescope

of the array is composed of three elements so that a good Z identification may be obtained in a large range of energies and Z values.

2. Apparatus design

The detector array operates in a vacuum vessel. It is placed at 50 cm from the target and, in the present configuration, it covers an angular range from $\pm 3^\circ$ to $\pm 23^\circ$ in and out of plane. The geometrical inefficiency is mainly due to the detector walls (25%), while the gaps left between the rows and columns of the detector modules account for only an additional 3% [10]. Around 0° the detecting system has a hole of $\pm 3^\circ$ to allow the beam to go through the array. To increase the efficiency in the very forward cone, four telescopes may be placed at 100 cm from the target, so that the central hole is reduced to $\pm 1.5^\circ$. This angle, however, can be easily varied, the choice depending on the beam optics quality and the grazing angle of the reaction to be studied.

The detecting system, shown in fig. 1, is based on 48 identical modules: their front surfaces are tangent to a sphere centered in the target. Each module, sketched in fig. 2, is shaped as a truncated pyramid (170 mm high) with square base and contains a three-detector

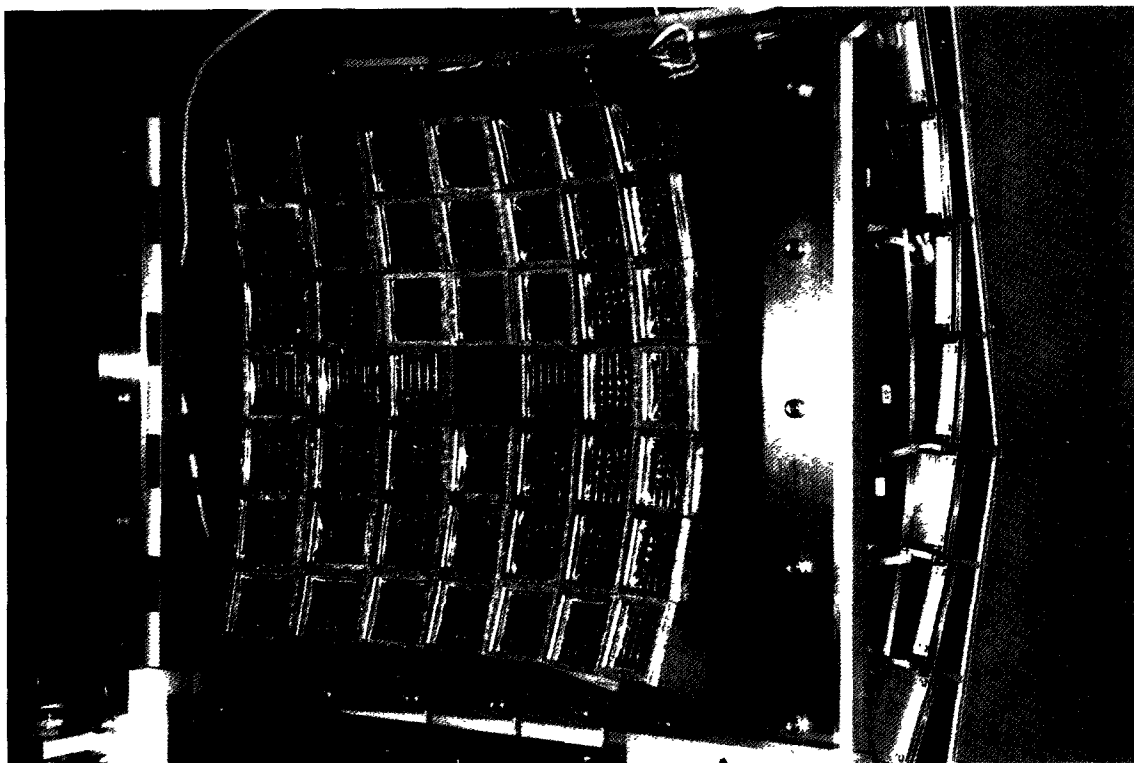


Fig. 1. View of the 48 modules mounted in the Nautilus chamber.

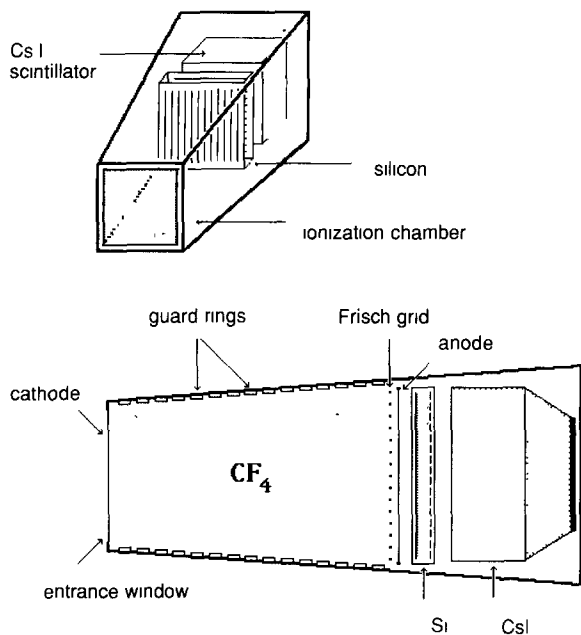


Fig. 2. Sketch of the three-element telescope.

telescope: a ionization chamber, a solid state detector (Si) and a scintillating crystal (CsI(Tl)).

The modules, closed on the rear side by metallic

structures which hold the telescope elements and allocate all the connectors, are inserted, in groups of three or four elements, on aluminium boxes which contain the preamplifiers, the valves for the gas flow regulation and the temperature and pressure transducers (fig. 3). The boxes lean on a rectified basement which is supported by a carriage that allows the position adjustment in three directions. A description of the detectors is reported in the following, while more details on the array construction can be found in ref. [8].

2.1. Ionization chamber

The pyramidal envelope of each module, for a length of 85 mm, is the ionization chamber (IC). The walls (2 mm G10 foils), externally coated with a golded layer acting as electrostatic shield, are assembled and vacuum sealed using an epoxidic glue. A channel, where the gas can flow and enter the IC very near the front side, is simply obtained in one of the walls overlapping two carved G10 sheets, thus avoiding any active area loss.

The ionization chamber is of the axial type as this configuration minimizes the active area loss. The entrance window ($42.4 \times 42.4 \text{ mm}^2$) is also the cathode; 36 golded Cu strips on the IC walls assure the uniformity of the electric field in the active volume. The Frisch

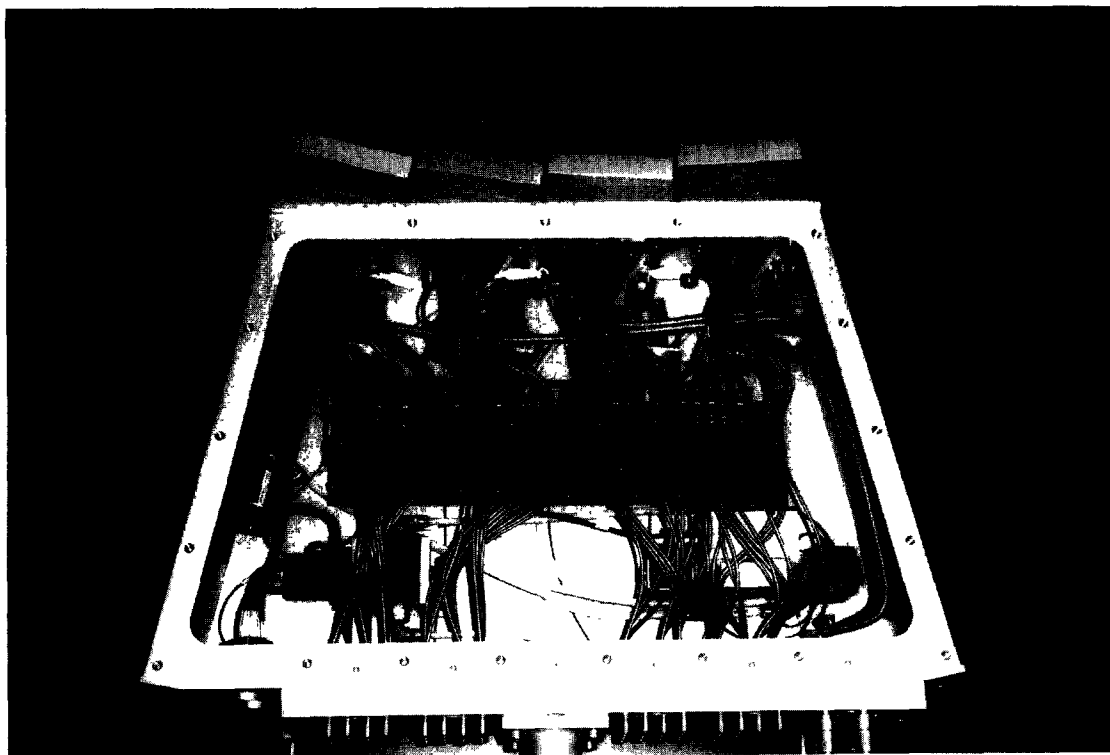


Fig. 3. View of the preamplifier, valve and transducer assembly.

grid and the anode define the active volume and are mounted on the rear cover. Whenever useful, the peculiar possibility [11] of the axial chambers to identify the atomic number of ions stopped in the active volume can be exploited. Ions of any Z value stop in the IC, operated at 200 mbar of CF_4 , for energy values lower than about 2.5 A MeV. Obviously lower thresholds can be set reducing the gas pressure. Tests on the signal to noise ratio have shown that even 70 mbar, corresponding to about 0.8 A MeV energy threshold, can be quite safely used. The CF_4 gas, continuously flowing in the detectors, has been chosen for the high density (0.837 mg/cm^3) and the high drift velocity ($10 \text{ cm}/\mu\text{s}$ at 1 V/cm/Torr). This last feature is important to reduce the electron collection times and the recombination rate between electrons and positive ions. The amount of gas in the detector volume is controlled through a VME based system [12]. The gas arrives at the detectors flowing through a filtering system, for oxygen and water vapor suppression, and through a cooling system. The gas outlet is controlled by a dry root pump and two compressors which allow the reuse of the gas (fig. 4).

Each detector has also on/off input and output valves, which can be closed through the remote control in case a particular detector has to be isolated. These valves are automatically closed in case of window breakage, which is notified to the central system by a special sensor apt to detect the inversion of the gas flow in the output tubing of any ionization chamber.

2.2. Silicon detectors

The silicon detectors, position sensitive in two coordinates, have an active area of $49.5 \times 49.5 \text{ mm}^2$ and a typical thickness of $500 \mu\text{m}$. Two different types have been tested and can be used.

The first one [13] is a strip detector, with 16 horizontal strips on one side and 16 vertical strips on the other side. The strips are connected on each side through 100Ω resistors to form resistive chains, at the end of which the signals containing the position information are obtained. The energy lost in the detector is given by the sum of the signals of any of the two chains. The main advantage of this type of silicon detector is that the position information, reflecting the strip structure, is discrete. No position calibration is thus required [14].

The second type of silicon detector has a resistive cathode [15]: the charge flowing to this electrode is divided by the resistive layer, as a nonlinear function of the position, in four signals available at the corners of the detector. A detailed study of the position determination [16] was convincing about the possibility of reasonably simple calibration. The energy loss information is given directly by the anodic signal. This fact and

the small reverse current, lower than in the previously mentioned type of detector, eventually give a better energy resolution. Obviously this is an advantage as the energy resolution is also important for the Z resolving power. Presently, only this second type of Si detectors is used in the apparatus.

The silicon detectors are mounted on G10 frames, designed to minimize the dead area (total dimensions $55 \times 57 \text{ mm}^2$). Three frames are used: the upper and the lower ones hold the detector in place and allocate the contacts while the intermediate frame has the function of avoiding any pressure to the silicon wafer. Eight pins are present on the silicon frame. Some are used by the silicon itself while others are for the anodic signal of the IC and to mechanically support the anode–Frisch grid block. All the pins find their appropriate connections on the frame supporting the CsI crystal.

The IC–Si telescope can stop about 8.5 A MeV He ions and 40 A MeV Xe ions.

2.3. CsI(Tl) scintillator

The CsI(Tl) scintillator has been chosen because of the advantages that it presents with respect to other possible candidates. It is only slightly hygroscopic so that hermetic sealing is not needed. Moreover it has good mechanical properties so that it can hold mechanical shocks fairly well and can be easily machined [17].

A high (4.51 g/cm^3) density makes this scintillator suitable to stop ions, in the energy range we are interested in, in a few centimeters. Furthermore the light emission spectrum fits well with the response curve of silicon photodiodes: the quantic efficiency is around 70% at 550 nm [18–20].

It is known that the specific light yield and the scintillation quenching depend on the charge, mass and energy of the particle. Therefore the energy calibration requires different ions at different energies. From the few data available the CsI(Tl) response function is a reasonably linear function of the ion kinetic energy above a given energy (5–6 A MeV) [21]. The dependence of the light output on the energy, however, has a slope that depends on the ion charge, decreasing with increasing Z value [22]. Experimental data for Z values up to Kr have been recently obtained [23]. No saturation of the light yield as a function of the deposited energy, has been reported up to now.

The crystals are 41 mm high and, for about 16 mm, are shaped as truncated pyramids, that act as light guides. The larger base is $51 \times 51 \text{ mm}^2$ while the smaller one ($25 \times 25 \text{ mm}^2$) is apt to be coupled to the photodiode. Photodiodes (PD) have been chosen because of various advantages. They require small space, have a good quantum efficiency for the CsI(Tl) light emission spectrum, are insensitive to magnetic fields,

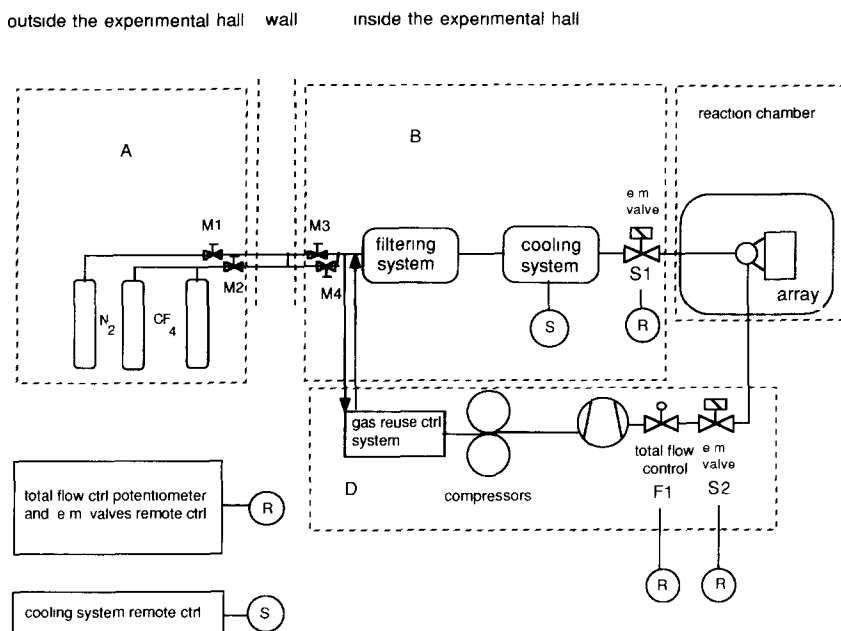


Fig. 4. Overview diagram of the gas system.

have a good gain stability and require low bias voltages. On the other side, the output signals are small, compared to signals from a photomultiplier, thus requiring careful handling to optimize the energy resolution.

We mounted the Hamamatsu S3204-05 photodiodes selected to have a dark current lower than 15 nA. The optical coupling is obtained using a two-component silicic glue that has a good transmission in the wavelength interval of interest and gives a stable contact even if it can be easily removed without any damage to the crystal or to the photodiode. The preamplifier for the PD signal is located inside the detector module, very near the crystal. The minimization of the distance between the PD and the preamplifier is in fact very important to have good performances.

As about 50% of the scintillation light may be lost through the lateral walls, particular care has been devoted to the treatment of these surfaces, that are properly polished and wrapped with teflon.

3. Signal processing and data acquisition

The signals from the detectors are handled by means of standard electronics chains for the pulse height analysis, based on charge preamplifier (PA), spectroscopy amplifier (SA) and analog to digital converter (ADC). A PA sensitivity of 1 mV/MeV(Si) is used for the silicon signals while 45 or 90 mV/MeV(Si) are used for the IC and PD signals. Particular care has been devoted, in the development of the board that

allocates the preamplifiers, to assure no detectable crosstalk. The amplifiers are built as four-fold units; the coarse and fine gains of any individual channel are controlled by a VME central unit. Shaping times of 1.5 μ s and 3 μ d are used for the IC, Si and PD respectively.

The signals from the silicon anodes and the photodiodes are also handled by fast amplifiers followed by constant fraction discriminators to generate triggers

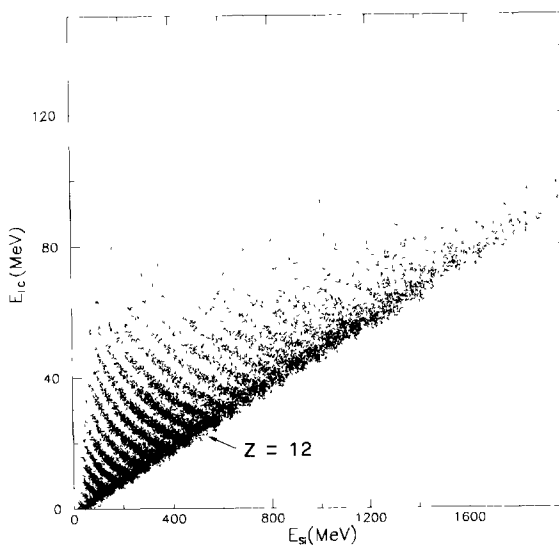


Fig. 5. Scatter plot of the IC energy loss vs the Si residual energy

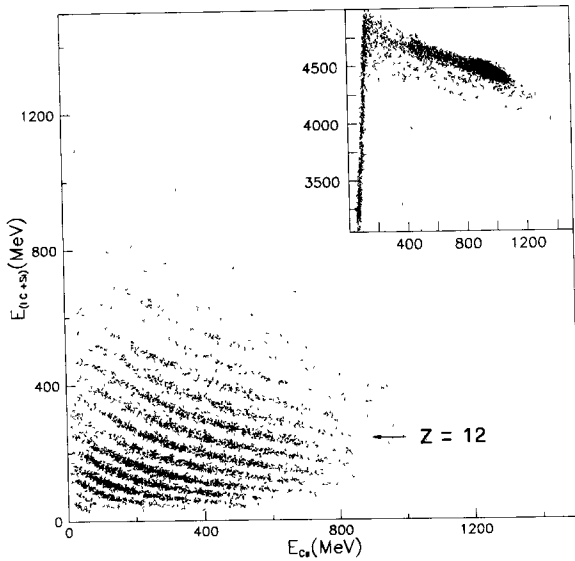


Fig. 6. Scatter plot of the IC+Si energy loss vs the CsI residual energy. In the insert the Z values around Xe are shown

and set the bit-pattern modules. A trigger to the data acquisition system is generated when at least one silicon detector has been fired. In this case all the signals of the telescopes corresponding to the silicon detectors whose bits are set in the pattern unit, are converted and stored, together with all the PD signals of any other telescope whose bit is set in the scintillator pattern units. The acquisition system used up to now is the GANIL system [24]. A system dedicated to the

apparatus is under development and is fully based on the VME standard, including ADCs and TDCs.

The main amplifiers [25], the ADC [26] and the TDC [27] as well as the PA [28], have been expressively developed by the Laboratory of Electronics of the Milano Nuclear Division and are commercially available.

4. Operation

The telescope array has been completely tested and it has been used at Ganil to investigate the IMF emitted in the Xe + Cu reaction at 45 A MeV. High voltage and permanent magnets were mounted on the target holder for electron suppression.

The energy resolution values, with 30.7 A MeV Xe beam, which is stopped in the Si detector, are 1% for the Si and 2% for the IC (293 MeV energy loss). The energy resolution value of the CsI, with 43.8 A MeV Ar beam, is 2.2%.

A scatter plot of the energy loss in the IC, runned at 200 mbar, vs the energy deposited in the Si detector, is reported in fig. 5. When ions punch through the silicon detector, the Z identification can be obtained considering the scatter plot of the IC + Si energy loss vs the residual energy in the CsI detector (fig. 6). The insert of fig. 6, which refers to the Xe + Au reaction, shows that even at $Z=54$ a reasonable Z identification can be obtained. No background subtraction has been applied to any shown spectrum.

The position calibration of the Si detectors is obtained following a procedure that has been described

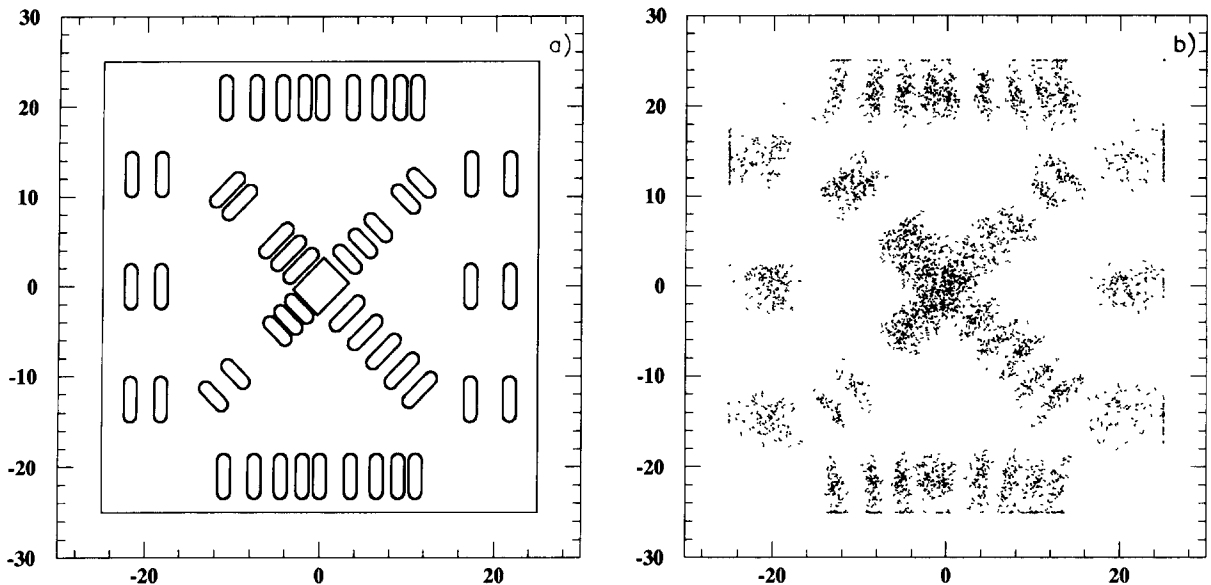


Fig. 7. (a) Mask shape and (b) the corresponding experimental xy distribution.

in detail elsewhere [16]. A screen, with holes coincident with the center of each Si detector, is placed in front of the apparatus. Thus, the gain of the amplifiers handling the four position signals are adjusted to give output signals of equal amplitude. The relationship between the signal and the position being not linear, the position resolution is worsening from the center to the periphery of the detector area. In these detectors and with the method applied, the position resolution ranges from 1 to 3 mm, corresponding to 0.1–0.3 degrees in our experimental conditions. An example of the position determination can be found in fig. 7, where the experimental data obtained with a mask are compared to the mask itself.

5. Conclusions

The design and performances of a IC–Si–CsI(Tl) telescope array have been presented. The array is particularly suitable for the detection of intermediate mass fragments and with the reverse kinematics technique. The three-element telescopes have a large dynamical range, low energy threshold, good charge and position resolution and can identify charges from light ions to at least $Z = 54$. The detector array has been used at Ganil to study the deexcitation of highly excited nuclear systems produced in intermediate energy heavy-ion reactions.

Given the modular structure of the detector array, some easy improvements are feasible and in progress. The angular coverage will be increased by adding two more columns of telescopes. A qualitative improvement, that is better charge resolution at high Z -values and easier energy calibration, will be achieved introducing, between the 500 μm Si detector and the CsI crystal, a 3.5 mm Si(Li) detector. Tests in this respect have already been made with very satisfactory results.

The detector array will be installed in the large scattering chamber Ciclope at the L.N.S. in Catania and will also be used in connection with light-particle and gamma ray detectors.

Acknowledgements

We thank the Ganil staff for their helpful support in the in-beam tests.

References

- [1] D.G. Sarantites et al., Nucl. Instr. and Meth. A264 (1988) 319.
- [2] J. Pouhot, Y. Chan, A. Dacal, A. Harmon, R. Knop,

- M.E. Ortiz, E. Plagnol and R.G. Stokstadt, Nucl. Instr. and Meth. A270 (1988) 69.
- [3] T. Murakami et al., Nucl. Instr. and Meth. A275 (1989) 112.
- [4] M.M. Fowler et al., Nucl. Instr. and Meth. A281 (1989) 517.
- [5] D. Drain et al., Nucl. Instr. and Meth. A281 (1989) 528.
- [6] D. Shapira et al., Nucl. Instr. and Meth. A301 (1991) 76.
- [7] K.L. Kehoe et al., Nucl. Instr. and Meth. A311 (1992) 258.
- [8] A. Moroni, I. Iori, L. Manduci, R. Scardaoni, S. Angius, A. Cortesi, L. Dellerà, G. Di Pietro, Sun Chongweng and Zhang Yuzhao, Report INFN/BE-91/06, 1991.
- [9] INDRA, B. Borderie, R. Dayras, J.L. Laville, R. Legrain; M. Louvel, E. Plagnol, E.C. Pollacco, J. Pouthas, M.F. Rivet, F. Saint-Laurent, J.C. Steckmeyer and C. Volant. GANIL report 89–10A, april 1989; N. Copinet, thesis, University of Caen, 1990.
- [10] M. Bruno, M. D'Agostino, P.M. Milazzo, S. Ostuni, E. Fuschini, and A. Moroni, Nucl. Instr. and Meth. A305 (1991) 410.
- [11] A. Moroni, I. Iori, Li Zu Yu, G. Prete, G. Viesti, F. Gramagna and A. Dainelli, Nucl. Instr. and Meth. 225 (1984) 57.
- [12] R. Bassini, C. Boiano, S. Brambilla, I. Iori, A. Moroni and Zhang Yinghi, Nucl. Instr. and Meth. A267 (1988) 499.
- [13] Micron Semiconductor, Lancing, England.
- [14] J. Walton, H. Sommer, G. Wozniak, O. Peaslee, D. Bowman, W. Kehoe and A. Moroni, IEEE Trans. Nucl. Sci. NS-37 (1990) 1578.
- [15] Intertechnique, Lingolsheim, France
- [16] M. Bruno et al., Nucl. Instr. and Meth. A311 (1992) 189.
- [17] H. Grassmann, E. Lorenz and H.G. Moser, Nucl. Instr. and Meth. 228 (1985) 323
- [18] I. Holl, E. Lorenz and G. Mageras, MPI-PAE/Exp E1.185, 1987.
- [19] H. Grassmann, H.G. Moser, H. Dietl, G. Eigen, V. Fonseca, E. Lorenz and G. Mageras, Nucl. Instr. and Meth. A234 (1985) 122.
- [20] P. Kreutz et al., Nucl. Instr. and Meth. A260 (1987) 120
- [21] D. Horn et al., Nucl. Instr. and Meth. A320 (1992) 273; G. Viesti, G. Prete, D. Fabris, K. Hagel, G. Nebbia and A. Menchaca-Rocha, Nucl. Instr. and Meth. A252 (1990) 75.
- [22] Ch.H. Pinkenburg, Entwicklung eines Hodoskops zur Messung von Kleinwinkelkorrelationen leichter Teilchen aus Schwerionenreaktionen, Diplomarbeit Univ. Frankfurt, 1989
- [23] N. Colonna, G.J. Wozniak, A. Veek, W. Skulski, G.W. Goth, L. Manduci, P.M. Milazzo and P.F. Mastnu, Nucl. Instr. and Meth. A321 (1992) 529.
- [24] Nouvelles du Ganil 34 (1990)15.
- [25] R. Bassini, C. Boiano, S. Brambilla, I. Iori, M. Malatesta and A. Moroni, Nucl. Instr. and Meth., to be published.
- [26] G. Bassato, R. Ponchia, R. Bassini and C. Boiano, IEEE Trans. Nucl. Sci. NS-37 (1990) 2185.
- [27] R. Bassini, C. Boiano, S. Brambilla and M. Malatesta, IEEE Nucl. Sci. Symposium, Santa Fe, New Mexico, Nov 1991, Abstract of papers, p. 38.
- [28] R. Bassini, C. Boiano, S. Brambilla, I. Iori, M. Malatesta and A. Moroni, Nucl. Instr. and Meth. A305 (1991) 449.